



Reinforcement Learning coupled with Finite Element Modeling for Facial Motion Learning

Duc-Phong Nguyen, Marie-Christine Ho Ba Tho, Tien-Tuan Dao

► To cite this version:

Duc-Phong Nguyen, Marie-Christine Ho Ba Tho, Tien-Tuan Dao. Reinforcement Learning coupled with Finite Element Modeling for Facial Motion Learning. Computer Methods and Programs in Biomedicine, 2022, pp.106904. 10.1016/j.cmpb.2022.106904 . hal-03676366

HAL Id: hal-03676366

<https://hal.science/hal-03676366v1>

Submitted on 22 Jul 2024

HAL is a multi-disciplinary open access archive for the deposit and dissemination of scientific research documents, whether they are published or not. The documents may come from teaching and research institutions in France or abroad, or from public or private research centers.

L'archive ouverte pluridisciplinaire **HAL**, est destinée au dépôt et à la diffusion de documents scientifiques de niveau recherche, publiés ou non, émanant des établissements d'enseignement et de recherche français ou étrangers, des laboratoires publics ou privés.



Distributed under a Creative Commons Attribution - NonCommercial 4.0 International License

Reinforcement Learning coupled with Finite Element Modeling for Facial Motion Learning

Duc-Phong NGUYEN¹, Marie-Christine HO BA THO¹, Tien-Tuan DAO²

¹ Université de technologie de Compiègne, CNRS, Biomechanics and Bioengineering,
Centre de recherche Royallieu, CS 60 319 - 60 203, Compiègne Cedex, France

² Univ. Lille, CNRS, Centrale Lille, UMR 9013 - LaMcube - Laboratoire de Mécanique,
Multiphysique, Multiéchelle, F-59000 Lille, France

duc-phong.nguyen@utc.fr, hobatho@utc.fr, tien-tuan.dao@centralelille.fr

Manuscript submitted as a **Research Paper** to the

Computer Methods and Programs in Biomedicine

(2nd Revision) May 2022

Corresponding author: Prof. Tien Tuan Dao

Centrale Lille Institut, CNRS UMR 9013 - LaMcube

Laboratoire de Mécanique, Multiphysique, Multiéchelle

59655 Villeneuve d'Ascq Cedex, France

Tel: 33 3 20 43 43 04

E-mail: tien-tuan.dao@centralelille.fr

20 Abstract

21 **Background and Objective:** Facial palsy patients or patients with facial transplantation have abnormal
22 facial motion due to altered facial muscle functions and nerve damage. Computer-aided system and physics-
23 based models have been developed to provide objective and quantitative information. However, the
24 predictive capacity of these solutions is still limited to explore the facial motion patterns with emerging
25 properties. The present study aims to couple the reinforcement learning and the finite element modeling for
26 facial motion learning and prediction.

27 **Methods:** A novel modeling workflow for learning facial motion was developed. A physically-based model
28 of the face within the Artisynth modeling platform was used. Information exchange protocol was proposed to
29 link reinforcement learning and rigid multi-bodies dynamics outcomes. Two reinforcement learning
30 algorithms (deep deterministic policy gradient (DDPG) and Twin-delayed DDPG (TD3)) were used and
31 implemented to drive the simulations of symmetry-oriented and smile movements. Numerical outcomes were
32 compared to experimental observations (Bosphorus database) for evaluation and validation purposes.

33 **Results:** As result, after more than 100 episodes of exploring the environment, the agent starts to learn from
34 previous trials and can find the optimal policy after more than 300 episodes of training. Regarding the
35 symmetry-oriented motion, the muscle excitations predicted by the trained agent help to increase the value of
36 reward from $R = -2.06$ to $R = -0.23$, which counts for ~89% improvement of the symmetry value of the face.
37 For smile-oriented motion, two points at the edge of the mouth move up 0.35 cm, which is within the range
38 of movements estimated from the Bosphorus database (0.4 ± 0.32 cm).

39 **Conclusions:** The present study explored the muscle excitation patterns by coupling reinforcement learning
40 with a detailed finite element model of the face. We developed, for the first time, a novel coupling scheme to
41 integrate the finite element simulation into the reinforcement learning for facial motion learning. As
42 perspectives, this present workflow will be applied for facial palsy and facial transplantation patients to guide
43 and optimize the functional rehabilitation program.

44 **Keywords:** Reinforcement learning, finite element modeling, facial motion learning, facial rehabilitation,
45 Artisynth.

1. Introduction

Facial palsy patients or patients with facial transplantation have abnormal facial motion patterns due to altered facial muscle functions and nerve damage leading to abnormal motion control for different movements such as eating, speaking, or facial expressions [1-4]. Moreover, involved patients also suffer asymmetric face effect, which indicates the imbalance and inequality of facial structure in terms of shape, size, location, and arrangement of left and right components on the sagittal plane [38]. In fact, the recovery of a symmetric face with balanced functionalities requires a complex rehabilitation process in which patients must practice patient specific facial movements. Thus, understanding of facial motion mechanism helps the involved patients to recover symmetrical movements and normal facial expressions. It is important to note that current facial rehabilitation has mainly based on a mirror approach to monitor the visual qualitative feedback from the rehabilitation exercise. More precisely, patients watch their distorted features in the mirror as a reference to teach themselves the right expressions during rehabilitation exercises. This strategy is ineffective and subjective without any feedback. Moreover, the current rehabilitation process is limited by a lack of patient specific knowledge about muscles driving facial motions. Therefore, understanding of facial motion mechanism and muscle activation and coordination is clearly fundamental. To provide quantitative and objective information on the facial motion during the rehabilitation exercise, computer-based systems that automatically recognizes action units (AUs) defined by the Facial Action Coding System (FACS) have been developed [5]. Such complex systems can provide an objective guideline for monitoring the facial rehabilitation process, which is a long-term, inconvenient, and sometimes ineffective [6-8].

In addition, for investigating muscles driving facial motion problem, biomechanical models are recommended because they can be customized to reflect the true anatomy and pathological anatomical deformations as well as imitate physical process [39]. In fact, physics-based facial models using finite element methods have been intensively developed to explore the role of the facial muscle excitation, contraction and coordination during facial motion [9-16, 31-32]. Muscle excitation represents the neural control process, which contracts the face tissues and moves the skull to perform facial expressions and movements. Despite a detailed view on the muscle contraction mechanism and its effect on the facial motion, the physics-based approach is descriptive with a priori known input information such as muscle properties. Moreover, which muscles and what value of muscle excitations for performing a desired movement for facial rehabilitation is still an open and longstanding research question. It is practically impossible to directly measure muscle activations from living subjects due to safety and accessibility limitations. Diverse numerical techniques have been proposed for estimating muscle excitation such as inverse dynamics, forward-dynamics tracking simulation, and optimal control strategies [10]. However, the use of this approach depends strongly on the a priori definition of input data, model properties and the targeted motion. Thus, this approach has a limited predictive capacity to explore a larger parameter space to find emerging properties during dynamic movements of the face.

In spite of the increasing availability of massive databases and computational models, artificial intelligence has rapidly grown [17]. One of the promising solutions in the control field is the reinforcement learning with tremendous theoretical and practical achievements in robotics control [18], gamming [19], autonomous driving [20], computer vision [21], and healthcare [22-24]. In particular, the question of the use of this learning strategy in the

healthcare domain to tackle real-world applications has recently raised [22-24]. Reinforcement learning distinguishes from other types of machine learning in several perspectives. The agent collects data through interactions with the environment and uses that data to train the agent itself. This dependence results in variation outcomes from one run to another. Recently, the reinforcement learning strategy has been coupled with rigid multi-bodies dynamics to explore the motion of the lower limbs during walking and age-related falls [33]. Thus, this learning strategy opens new avenues to explore human system motion and novel emerging properties without any a priori motion data. Thus, the present study aims to explore the facial motion learning capacity by the coupling between the reinforcement learning and the finite element modeling. The main objective is to provide, for the first time, the modeling workflow for this complex coupling and then to evaluate different learning strategies to establish motion patterns of the face during facial expression motions. Our novel solution will explore the patient specific facial motions without a priori data from the patient and then provides a set of facial muscle activation and coordination patterns for a specific rehabilitation-oriented movement (e.g. symmetry or smile). The remainder of the paper is organized as follows: section 2 focuses on the coupling workflow between reinforcement learning and finite element model of the face for learning symmetry and smile motions. Section 3 provides computational results and the comparison with other studies. Section 4 provides a detail discussion on the method and obtained results. Finally, section 5 addresses conclusions and perspectives of the present work.

2. Materials and methods

2.1 Novel coupling workflow between reinforcement learning and finite element modeling

Our novel simulation workflow requires main two components (Fig. 1): 1) A reinforcement learning agent (a human face) having a policy that decides what action (muscle excitations) to take when it observes a state (facial motion) and 2) A finite element modeling and simulation environment. The coupling between the finite element simulation environment and the reinforcement learning process is managed by an information exchange protocol. More precisely, at the beginning, the reinforcement learning agent observes the state of the face using the positions of selected key points (Fig. 2). Secondly, the policy predicts values of muscle excitations, which are then applied to the biomechanical model of the face for a physical simulation. Then, the simulation environment returns the positions of selected key points after simulation. And finally, these positions are used to compute the reward value by pre-designed multi-objective function (related to symmetry or smile exercises), which is then used to update training parameters for the training process.

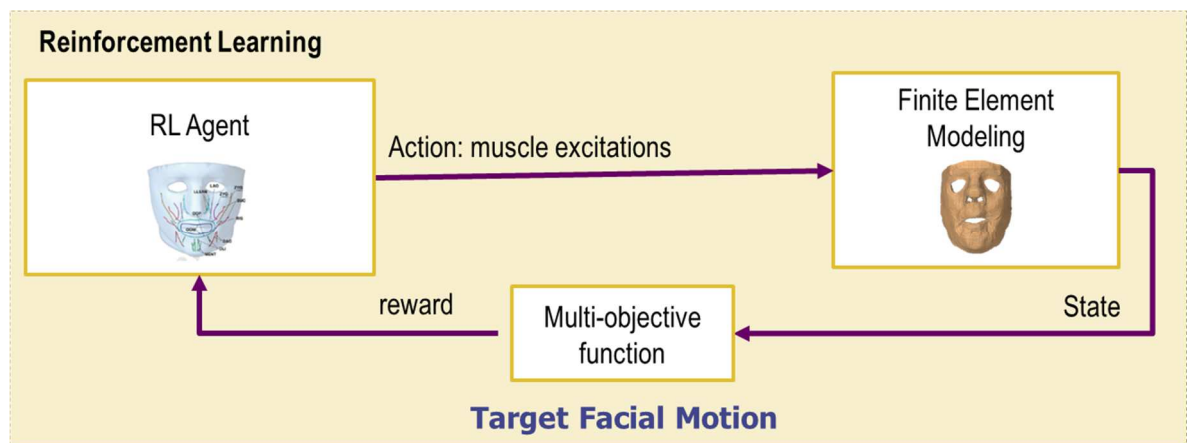


Figure 1. Overview of the novel coupling workflow between reinforcement learning and finite element modeling.

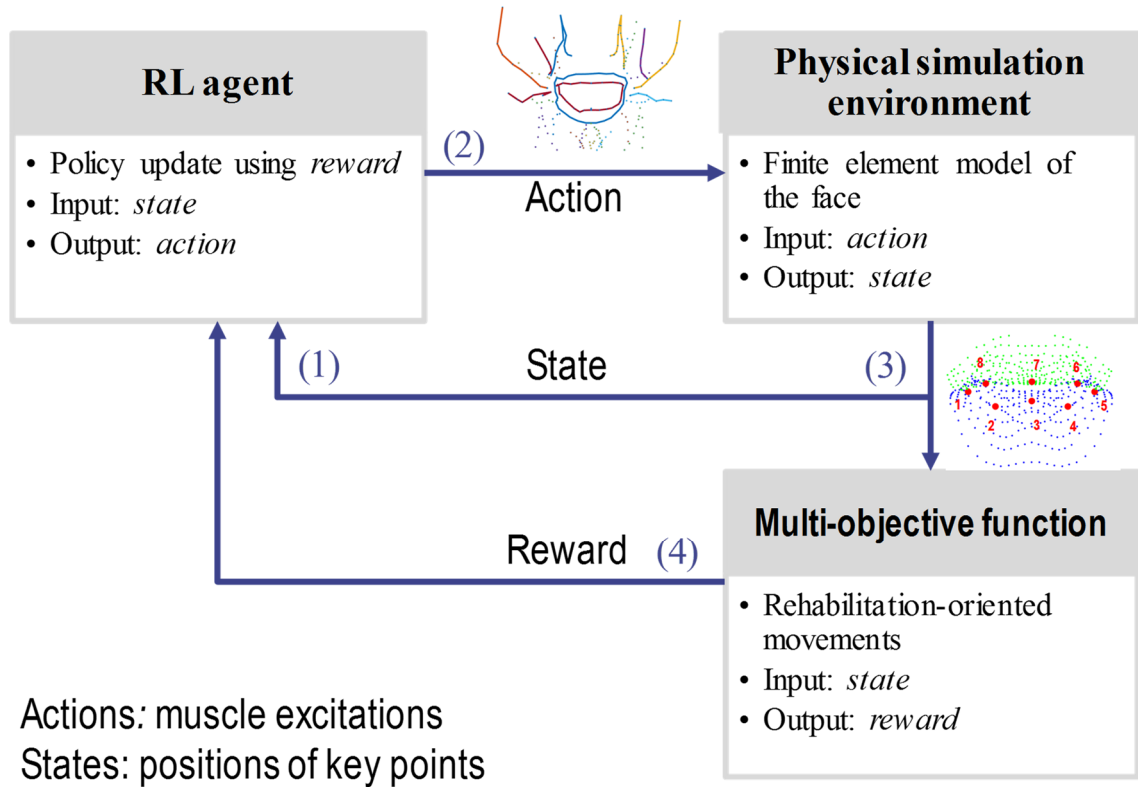


Figure 2. Detailed flowchart of the interaction between reinforcement learning and finite element modeling processes.

2.2 Face finite element model

A physically-based model of the face within the Artisynth modeling platform was used (Fig. 3a). This model has been from previous researches [16], [25], [26], [27]. The face finite element model includes three components such as 1) soft-tissue component with the hypodermis, dermis, and epidermis layers, 2) a cranium and maxilla component, 3) a jaw-hyoid component [28]. To reduce computational cost and accelerate the training process, the facial model is simplified by keeping only the soft-tissue component with ten orofacial muscles (Levator Anguli Oris (LAO), Levator Labii Superioris Alaeque Nasi (LLSAN), Buccinator (BUC), Zygomaticus (ZYG), Depressor Anguli Oris (DAO), Risorius (RIS), Depressor Labii Inferioris (DLI), Mentalis (MENT), Orbicularis Oris Peripheralis (OOP),

Orbicularis Oris Marginalis (OOM)) (Fig. 3c). The soft tissue finite element mesh consists of 6342 brick elements (with 6024 hexahedrons and 318 wedges) and 8720 nodes. The activation for the face model results from the orofacial muscle strain and force. Ten orofacial muscles are modeled and attached in the lower face that applies muscle forces in terms of muscle excitations onto the finite element model. Muscle fibers are modeled by a set of uniaxial cable elements. For example, the zygomatic ligaments are represented by fixing all degrees-of-freedom of soft tissue nodes that are in the region where these ligaments attach to the maxilla. Soft tissue constitutive equation for the hypodermis layer is based on a Mooney-Rivlin constitutive equation, and Fung constitutive equation for the epidermis and dermis layer as in the Flynn et al. paper [16]. The mechanical characteristics (such as force-displacement response, pre-stress behaviors, non-linear, anisotropic, and viscoelastic constitutive laws) for the skin layer were estimated based on a combination of in vivo experiments and numerical methods. Muscles are modeled as continuous sets of cable elements, which activate in tension as point-to-point Hill-type models and are aligned along element edges. The mechanical property evolution of muscle contraction comprises muscle contractile fibres (active part), muscle body (passive part), and the stress stiffening effect [25]. The movements of the mandible generated by muscles of mastication are not handled yet in the model. Thus, the superficial muscles, which are muscles around the lip region, involved in facial mimics are focused. Two finite element models of the face corresponding with the modeling of the symmetric face (Fig. 3a) and the asymmetric face (Fig. 3b).

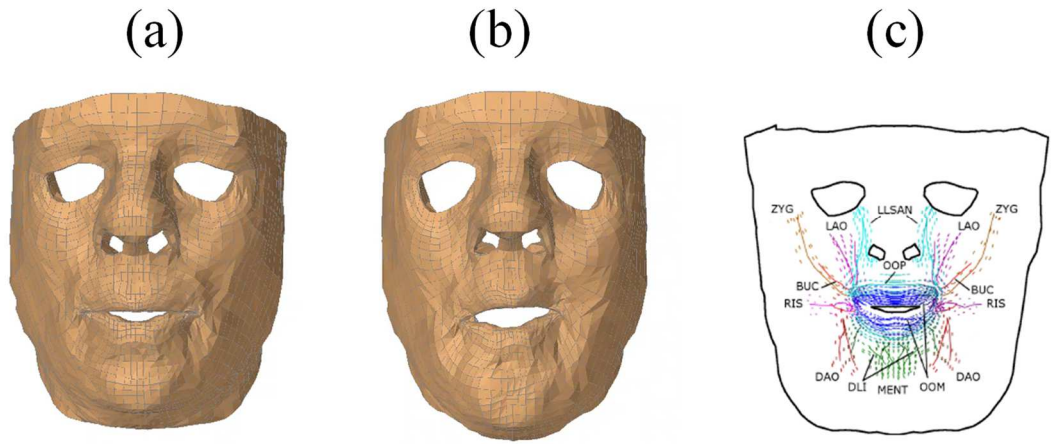


Figure 3. The face finite element model (a) referred as the symmetric face, (b) referred as the asymmetric face (unbalanced deformation between left and right sides), and related facial muscle network (c).

2.3 Reinforcement Learning for Facial Motion Control

2.3.1 Reinforcement learning model and algorithms

Reinforcement learning (RL) aims to find a policy, $\pi(a|s)$, which maps the state space to the action space and instructs the agent on how to make decisions that maximizes the long-term cumulative reward inspired by a reward function $r(s, a)$, where a is the action needs to take in the state s . Bellman equations are solved to find the optimal policy. In this present study, two RL algorithms were used. The first algorithm is the Deep Deterministic Policy Gradient (DDPG) in which the Bellman equation was solved by combining a deep neural network for learning Q function and a deterministic policy gradient algorithm for learning a policy. This is off-policy reinforcement learning used for continuous state and action spaces, which is suitable for our problem. The second used algorithm is the Twin Delayed DDPG (TD3). DDPG is often brittle with the tuning process for hyperparameters. It usually fails when exploiting the error in the Q-function, the learned Q function starts to

overestimate Q-values results in policy breaking. Twin delayed DDPG copes with this issue and improves performance by applying three tricks as 1) Clipped Double-Q Learning: learning two Q-functions (twin) and using smaller Q-values for the Bellman error loss functions, 2) Delayed Policy Updates: sparse updating the policy compared to the Q-function, 3) Target Policy Smoothing: adding noise to target actions to reduce exploiting Q-function errors.

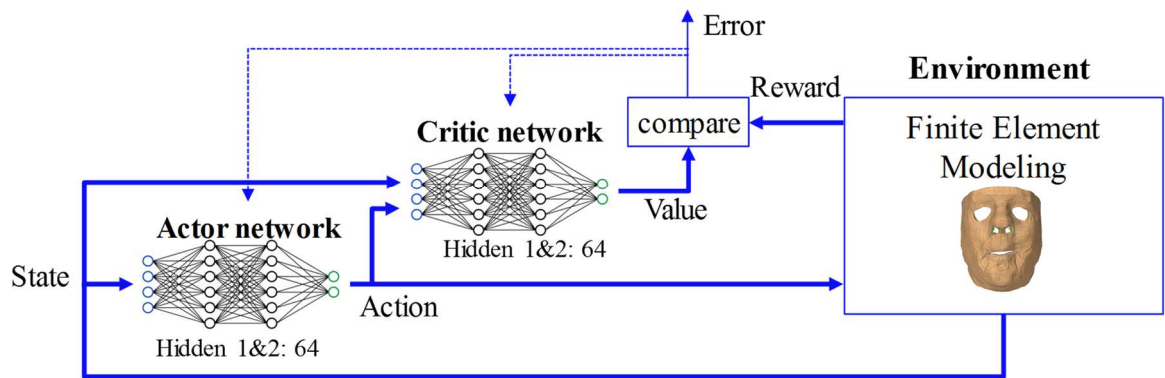


Figure 4. The network architecture of DDPG: one actor network and one critic network.

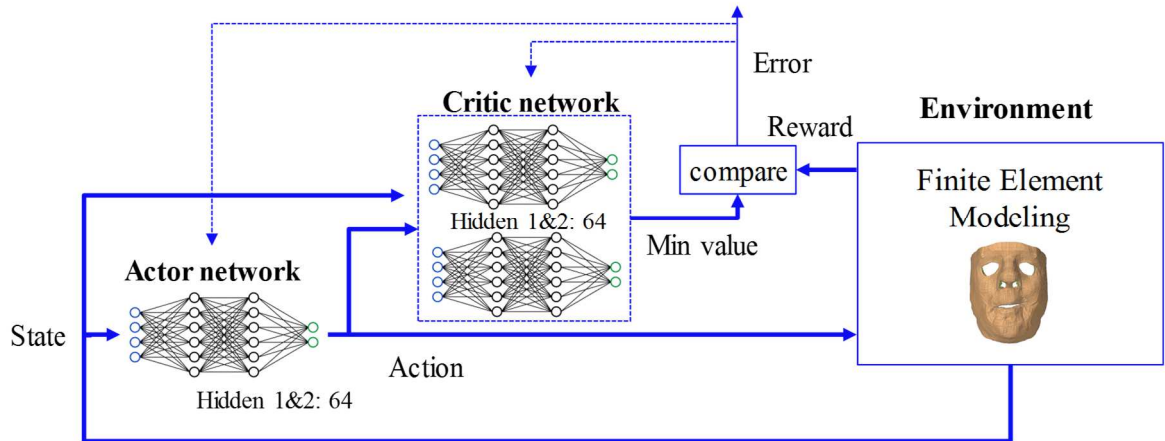


Figure 5. The network architecture of TD3: one actor network and two critic networks.

The network architecture of DDPG contains the actor network and the critic network. Each network has two hidden layers with 64 nodes (Fig. 4). The actor network inputs the state vector while outputs the action vector. The input of the critic network contains both the

action vector output from the actor network and the state vector, while the output is the predicted Q-value. TD3 has the same architecture as in DDPG except it has two critic networks (Fig. 5).

2.3.2 Reward Function, Action Space, and State Space

The aim of our study is to find the appropriate muscle excitations for performing a facial motion, which is generated by defining appropriate biomechanics-inspired reward function. In our model, action is a vector of 10 pairs of left and right muscles in terms of muscle forces normalized between 0 and 1. To avoid the exhausted search, only significant muscles (*left and right Levator Anguli Oris (LAO)*, *left and right Levator Labii Superioris Alaeque Nasi (LLSAN)*, *left and right Zygomatics (ZYG)*, *left and right Risorious (RIS)*, *Orbicularis Oris Marginalis (OOM)*, *Orbicularis Oris Peripheralis (OOP)*) were included in training process (Fig. 6a). In our model, the agent's state was defined through a set of landmark points focusing on the mouth region of the face. In fact, 8 key points on the lips are chosen as representations of the state of the face (Fig. 6b).

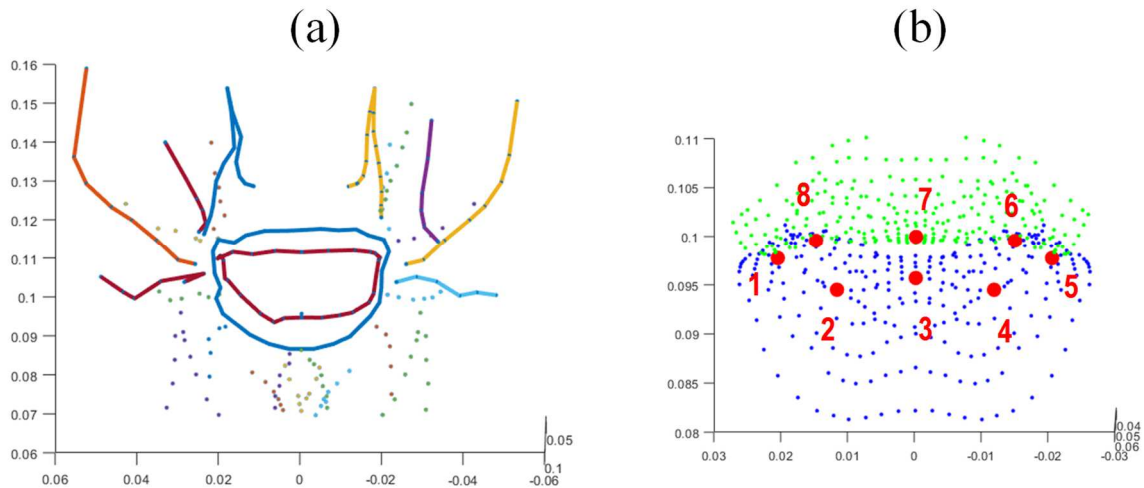


Figure 6. Selected muscles excitations for training (a) and landmark points for the RL agent's state (b).

Regarding the reward function, the agent receives a reward value from environment at each time-step. Note that the training efficiency of reinforcement learning algorithm depends strongly on defining the reward function. In our study, the reward function is designed by a motion-oriented (e.g. symmetry-targeted motion, smile expression, sound pronunciations) strategy. More precisely, different reward functions were formulated using the Euclidean distance and angle created from the defined 8 landmark points. Mathematically, reward functions are defined as follows:

$$R_{symmetry}^{distance} = -1000 * (r_1^d + r_2^d + r_3^d) \quad (1)$$

$$R_{symmetry}^{angle} = -(r_1^a + r_2^a + r_3^a) \quad (2)$$

$$R_{smile} = \Delta d \quad (3)$$

where r_i^d, r_i^a are the symmetry value-based distance and angle between left side compared to right side for each pair point (point 1-5, 2-4, 8-6). Δd is the total moving up of point #1 and point #5 defined in Fig. 6b.

2.4 Information exchange protocol and implementation

Our study is based on two modeling platforms (i.e. Artisynth and PyTorch) coming from different fields. The exchange information between these platforms need a novel communication protocol. Artisynth-RL has been proposed to open the exchange capacity with rigid multi-bodies dynamics simulation [30]. In the present study, Artisynth-RL was extended to exchange information between the PyTorch platform which is a Python-based training platform for RL models and Artisynth for running face finite element simulation. Note that Artisynth-RL is a cross-platform based java script. To achieve this objective, different technologies (RESTful API as a plugin, Spark framework from java, and Request

package from python) were used as shown in Fig. 7. Regarding the communication protocol, the muscle excitations from the reinforcement learning module are posted into the Artisyng module, then a new state is obtained from the Artisyng module to reinforcement learning module after each simulation step.

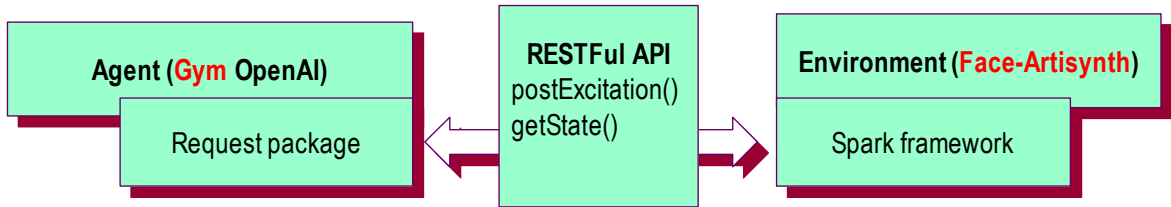


Figure 7. RESTful API as a plugin for bridging reinforcement learning and Artisyng

As hardware configuration, a virtual machine configuration with ubuntu 20.04, 8 CPU, 16 Gb RAM, Python 3.6, and the open-source stable-baselines3 was used for the training process.

2.5 Evaluation and validation

An open access 3D face database, named Bosphorus, was used for evaluation and validation purpose. This database includes 105 subjects (44 females and 61 males) with different expressions, poses, and occlusion conditions. 65 subjects have 7 expressions such as happiness (smile), surprise, fear, sadness, anger, disgust, and neutral. Happiness (smile) and neutral expressions, which are available in 130 face scans of all the subjects, were used for further validation. Firstly, three key point at positions #1, #5, and #7 (as in Fig. 6b) were manually picked for each face scan. Secondly, all the face scans were transferred such that the point at position #7 is at the origin (coordinate [0, 0, 0]) and face scans of the same person is at the same orientation. Finally, the total displacement of moving up action of the two key points at positions #1 and #5 (as in Fig. 6b) were computed by subtracting the corresponding points of smile face scan and neutral face scan of the same person. In

fact, the values of the used reward functions were computed for each posture (neutral and smile expression). Obtained values were represented in mean and standard deviation and then compared to the final outcomes from the RL process.



Figure 8. Illustration from Bosphorus database with two expressions: neutral (left) and smile (right).

A hyperparameter tuning process was implemented to select the best neural network architecture and parameters. In particular, the hyperparameter tuning process is not automatically tuned, but manually selects each parameter, while other parameters remain unchanged. Each trial was performed for a training task with the hyperparameter within a predefined set to ensure that the agent successfully explores and learns to make decisions in its environment. The predefined set of hyperparameters includes several most critical parameters, which govern the performance of reinforcement learning such as the neural network size (nodes in hidden layers ([64, 64] or [400, 300] for the actor and the critic networks)), learning rate (0.001, 0.01, note that the learning rate is shared for all networks), batch size (16, 32), τ parameter, which used to soft update both critic and actor target networks (0.001, 0.005).

3. Computational results

3.1 RL accuracy and performance

Figure 9 shows the reward and the loss evolutions during the training process of the agent to conduct one symmetry action. In general, after more than 100 episodes of random interaction in the environment, the agent starts to learn from previous trials and can find the optimal policy after more than 300 episodes of training. In particular, the learning start parameter was set to 100 in the training phase, allowing the reinforcement learning agent to collect a set of transitions ($\mathcal{D} = (s, a, r, s', d)$) by performing a random action from the action space to the environment before learning from previous trials. These random actions result in instable trend in the reward values in first 100 episodes. Having just 200 episodes of learning, the agent still learns and explores the environment to discover the optimal policy. During learning, the not optimal policy may predict the random actions for exploring more the environment that might dramatically drop reward values. From 200 to 300 episodes of learning, the agent gradually finds the optimal policy after more than 300 episodes of training. The reduction in actor loss and critic loss values demonstrates the efficacy of learning strategy in both DDPG and TD3 methods. The reward value predicted using the model trained by TD3 ($R = -0.26$) is slightly higher than that of using the model trained by DDPG ($R = -0.33$).

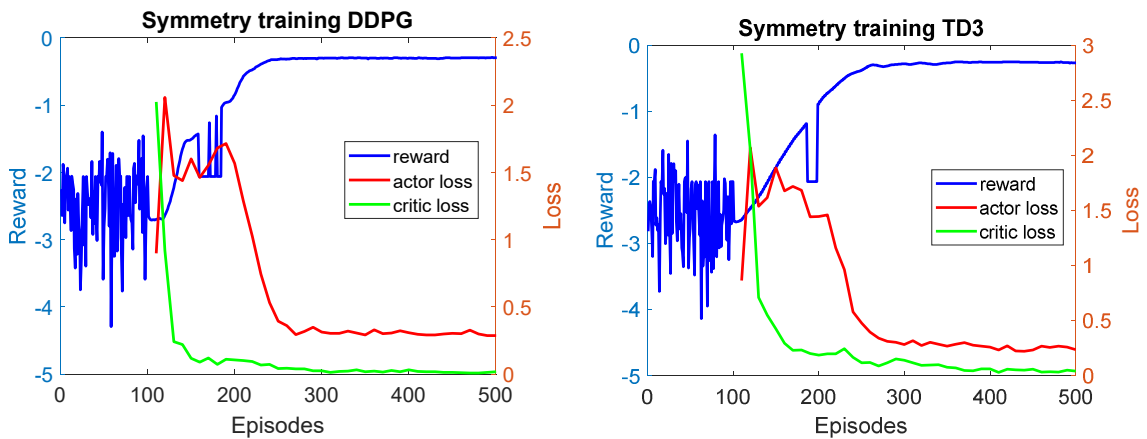


Figure 9. The reward value and the loss values of the actor network and the critic network during training reinforcement learning agent with two different methods: DDPG (left), TD3 (right) for symmetry-oriented functional rehabilitation using 4 muscles as ZYG, RIS, OOM, OOP. The reward value predicted using the model trained by DDPG is $R = -0.33$. The reward value predicted using the model trained by TD3 is $R = -0.26$.

Figure 10 shows the reward and the loss evolutions during the training process of the agent to perform the smile action. The similar patterns are observed according to figure 9. More precisely, the agent spends 100 episodes collecting a set of transitions by taking random actions to the environment resulting in instability of reward values. It then starts to learn from previous trials and can find the optimal policy after more than 200 episodes of training. The training is successfully demonstrated by the reduction of the loss value of both actor and critic networks. The reward values during training model using DDPG algorithm seem noisier compared to that of training model using TD3 algorithm. The reward value predicted using the model trained by TD3 ($R = 5.36$) is slightly higher than that of using the model trained by DDPG ($R = 5.26$).

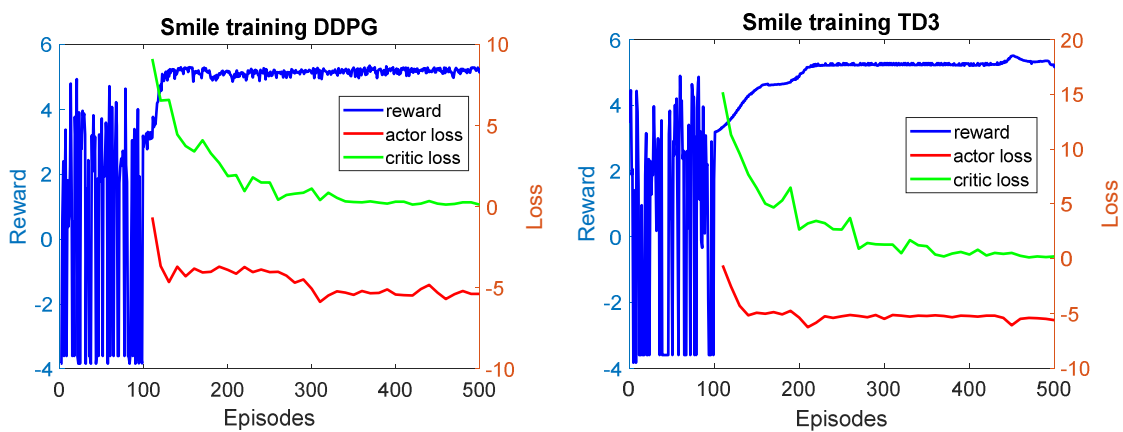


Figure 10. The reward value and the loss values of the actor network and the critic network during training reinforcement learning agent with two different methods: DDPG

(left), TD3 (right) for smile-oriented functional rehabilitation using 3 facial muscles as LAO, LLSAN, ZYG. The reward value predicted using the model trained by DDPG is $R = 5.26$. The reward value predicted using the model trained by TD3 is $R = 5.36$.

Table 1 shows the reward values obtained during the hyperparameter tuning process for DDPG method when training smile expression. The process can help to identify the better network architecture with associated optimal set of hyperparameters. In fact, the reinforcement learning architecture including two hidden layers [400, 300] for the actor and the critic networks, a batch size of 16, a learning rate for all networks of 0.001, τ parameter of 0.005, and without action noise yields the best reward value. The computational time for training 500 episodes for each smile training and symmetry training is around 6 hours. However, the most computational time is in the simulation environment, where each simulation lasts for 30 seconds (5 hours for 500 episodes related to simulation and restart of Artisynth only). Figure 11 reports the effect of the network architecture and τ parameter. The network architecture has a more important effect than that of the τ parameter.

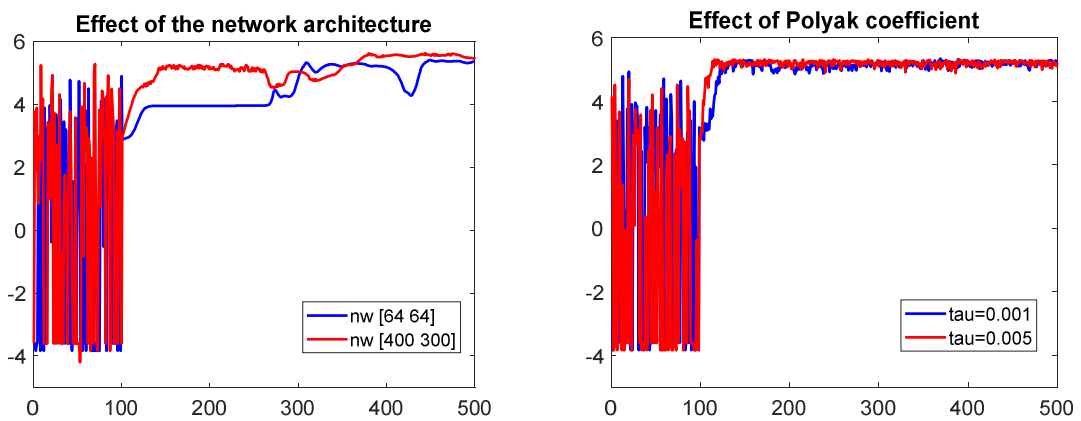


Figure 11. Reward value during training reinforcement learning agent with different hyperparameters and the network architecture.

Table 1. The reward values obtained during the hyperparameter tuning process		
Hyperparameters		Reward
Batch size	16	5.21
	32	5.16
Learning rate	0.01	4.59
	0.001	5.35
Network architecture	[64, 64]	4.81
	[400, 300]	5.45
τ parameter	0.001	5.22
	0.005	5.26
Action noise	With	4.69
	Without	5.35

To sum up, two reinforcement learning algorithms namely DDPG and TD3 have been used for learning symmetry and smile motions of the finite element model of the face. In terms of reward predicted from the trained model, TD3 seems to have slightly better performance compared to DDPG. The hyperparameter tuning process was also proposed to find the suitable parameter for the model.

3.2 Facial motion learning

The obtained outcome and corresponding muscle excitation value of the symmetry-oriented functional rehabilitation is shown in Fig. 12. and Table 2. According to the prediction, the muscle on the right side of the mouth such as right OOM, right RIS, and right ZYG are activated, while only the left OOP muscle is activated to improve the symmetry of the face from the initial state with the reward value $R = -2.06$ to the new state with the reward value $R = -0.23$, which counts 88.8% improvement.

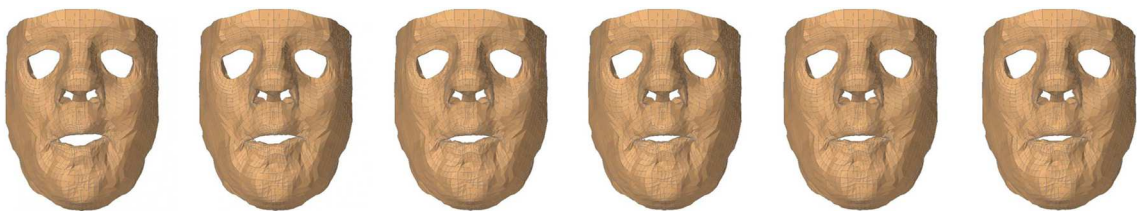


Figure 12. Face animation for symmetry-oriented motion. The face at initial state (on the left $R = -2.06$) and after received muscle excitation (on the right $R = -0.23$) output from reinforcement learning for symmetry-oriented functional rehabilitation.

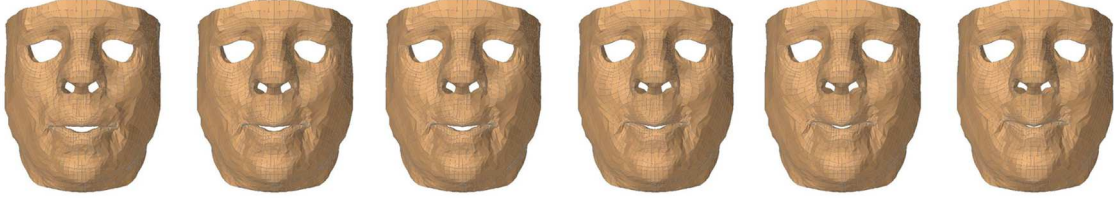


Figure 13. Face animation for smile-oriented motion. The face at initial state (on the left $R = -1.6$) and after received muscle excitation (on the right $R = 5.35$) output from reinforcement learning for smile-oriented motion.

Regarding the smile-oriented motion simulation of the finite element model of the face, both left and right muscles of LAO and ZYG are activated, while LLSAN is not activated as in Fig. 13 and Table 3. The measured reward value increases from -1.6 at the initial state to 5.3 at the terminal state. The obtained muscle activation levels for smiling movement are within the range of values reported by Flynn et al. [16]. However, it is important to note that there is a difference in smiling patterns between our simulation (i.e. unconstrained smile) and their simulations (i.e. smiles with open mouth or closed mouth).

The muscle action line length change and contraction amplitude $\xi^{CE} = \frac{L-L_0}{L_0} = \frac{\Delta L}{L_0}$ are shown in Table 2. The contraction amplitudes of OOM and OOP are estimated as the area that these muscles cover $\xi^{CE} = \frac{S-S_0}{S_0} = \frac{\Delta S}{S_0}$. Related to the smile, the right ZYG contracts -16.26%, while this number on the left is -15.12%. The right and left LAO contract around -30%. Note that all muscle contraction levels during smiling are in good agreement with those estimated using Kinect-driven rigid multi-bodies modeling (Nguyen et al. [40]). In

their study [40], the head model was reconstructed from the subject-specific data acquired by a Kinect device in a smile position. Then, a skull model was generated using the statistical fitting method from a generic skull model and the head model. Moreover, a muscle network was defined using insertion points on the head model and attachment points from the skull model. Finally, the muscle contraction levels were estimated using the length of these insertion points and attachment points.

Table 2. Muscle contraction levels during different facial expressions and comparison to the literature data.

Muscle / ξ^{CE}	symmetry		Smile		Nguyen et al. [40] (smile)
	L_0 (mm) / S_0 (mm ²)	$\frac{\Delta L}{L_0}$ (%) / $\frac{\Delta S}{S_0}$ (%)	L_0 (mm) / S_0 (mm ²)	$\frac{\Delta L}{L_0}$ (%) / $\frac{\Delta S}{S_0}$ (%)	$\frac{\Delta L}{L_0}$ (%)
Right ZYG	52 mm	-2.19	54.5 mm	-16.31	From -9.13 to -19.72
Left ZYG	52.2 mm	1.12	54.6 mm	-15.09	From -13.59 to -21.32
Right LLSAN	27.2 mm	-1.62	27.9 mm	-10.26	From -1.99 to -8.12
Left LLSAN	27.2 mm	-0.38	27.9 mm	-10.2	From -0.69 to -6.13
Right LAO	27.3 mm	-1.18	30 mm	-28.13	From -18.66 to -29.46
Left LAO	24.3 mm	1.56	30 mm	-28.17	From -21.19 to -28.03
Right RIS	52.2 mm	-6.21	52.9 mm	-8.12	From 3.55 to 7.30
Left RIS	52 mm	2.44	52.9 mm	-8.135	From -3.09 to 6.96
OOM	590 mm ²	-12.97	665 mm ²	-2.01	-
OOP	1099 mm ²	-7.98	1138 mm ²	17.40	-

Table 3. Muscle activation levels reported from our simulation and its comparison to the literature data

Muscle	symmetry	smile	Flynn et al. [16] (closed mouth smile)	Flynn et al. [16] (open mouth smile)
Right ZYG	0.2	0.4	0.2	0.5
Left ZYG	0	0.4	0.2	0.5
Right LLSAN	0	0	0.1	0.5
Left LLSAN	0	0	0.1	0.5
Right LAO	0	0.4	0.1	0.5
Left LAO	0	0.4	0.1	0.5
Right RIS	0.4	0	0.2	0.6

Left RIS	0	0	0.2	0.6
Right OOM	0	0	0	0
Left OOM	0	0	0	0
Right OOP	0.1	0	0	0
Left OOP	0.4	0	0	0

3.3 Evaluation and validation

For symmetry-oriented motion, the muscle excitations predicted by the trained agent help to increase the value of reward from $R = -2.06$ to $R = -0.23$, which counts for $\sim 88.8\%$. While this number for smile-oriented motion, the reward value for both corners of the mouth increases from $R = -1.6$ at the initial state to around $R = 5.3$ at the terminal state, which is 0.35 cm moving up on average for each corner of the mouth. The average distance of moving up for each corner of the mouth was 3.4 ± 0.2 estimated using reward values from Table 1 for different hyperparameters of the reinforcement learning algorithm. This is within the range of movements compared to the value calculated from the Bosphorus database, this value is 0.4 ± 0.32 cm when a person makes maximum effort to smile as in Fig. 14. The variation in the value of this displacement of the Bosphorus database is large (0.32 cm) compared to our results (0.02 cm). This is due to this value being estimated from 65 different subjects, while our result was only estimated using one patient-specific model of the face.

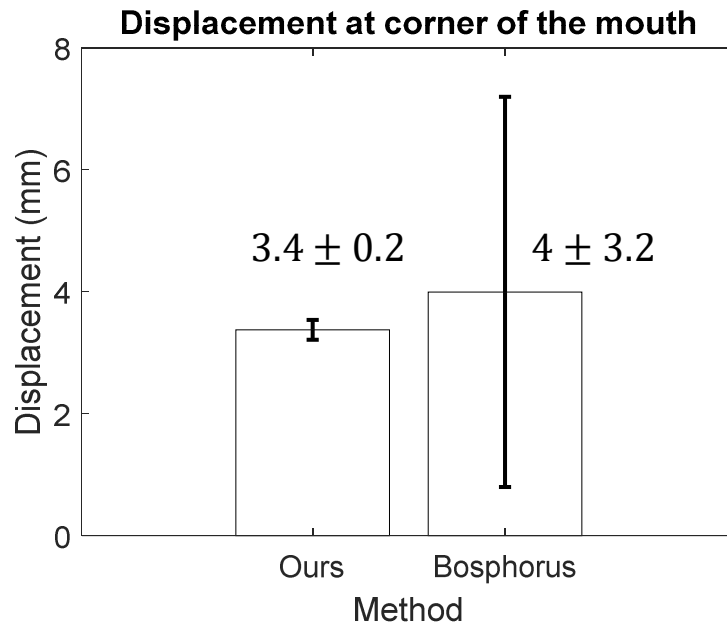


Figure 14. Displacement of the corner point of the mouth (moving up direction) of our method and from the Bosphorus database of the smile position compared to the neutral position.

4. Discussion

Understanding muscle coordination mechanism of facial expressions plays a crucial role in the facial rehabilitation interventions for facial palsy or facial transplantation patients. Numerical models (i.e. finite element models) have been intensively developed [31] to provide a better understanding of this complex process. However, these developed models are descriptive and their predictive capacity is still limited. Besides, computer-based monitoring systems, that automatically recognize action units (AUs) to provide quantitative and objective information on the facial motion during the rehabilitation exercise have been developed [5, 36, 37]. Despite many efforts, understanding of facial motion mechanism still remains a scientific and clinical challenge to help the involved patients to recover functional facial movements. In particular, the role of muscle excitation

and its value for performing a desired facial movement for facial rehabilitation is still an open and longstanding research question. To achieve this complex and challenging objective, the present study aimed to couple reinforcement learning approach to a muscle-driven biomechanical model of the face to explore the facial motion learning capacity such as symmetry and facial smiling actions. For the first time, facial expressions (e.g. smile) are simulated without a priori input data (e.g. motion capture data). In fact, our novel coupling scheme allows to explore emerging properties of the facial muscle contraction mechanism and guides iteratively the face to express smiling action or becomes a symmetric face. Thus, obtained outcomes showed the potential application of this novel approach with facial palsy patients for a better understanding of facial muscle coordination and muscle activation patterns to target a specific motion.

More precisely, regarding the symmetric motion of the face, the muscle contraction involves right OOM, right RIS, and right ZYG, while only the left OOP muscle is activated. This is reasonable due to the physical-based model of the face used for symmetry training is drooping of the mouth on the right side. From the biomechanics point of view, this is a symptom of the facial palsy patient on the affected side of the face. In smile-oriented motion of the face, levator anguli oris and zygomaticus are the main muscles responsible for smile action resulting in two corner points in the mouth moving up 0.35 cm, which is within the range of motion compared to the Bosphorus database (0.4 ± 0.32 cm). There is also a good agreement in muscle involvement for smile training as LAO and ZYG compared with the simulation of Flynn et al. [16]. Note that Flynn et al. manually adjusted muscle excitation value to find the appropriate value for expression movements of the finite element model of the face. In fact, our present study revealed the usefulness of the mechanical modeling coupled with reinforcement learning to guide the design of patient

specific precision rehabilitation for the face with muscle activation and coordination mechanisms.

Recently, deep reinforcement learning becomes an interesting solution for complex control problems [33]. The coupling between a reinforcement learning strategy and a deep neural network allows the agent to build knowledge by gathering information while interacting with the environment. In fact, no prior data is required for training. This particular character enhances the predictive capacity of the involved model. Indeed, reinforcement learning methods were used to solve our problem since they require no prior input data (i.e. muscle excitation and activation patterns). This is particularly useful for learning muscle-driven facial motion problems. While other learning approaches require a database for training, collecting experimental data by directly measuring muscle excitations from living subjects is hard or impossible due to safety and accessibility limitations [9]. One of the challenges when developing an efficient RL model relates to the use cumulative rewards to quantify how the agents ought to take actions in an environment. In our present study, specific rewards were defined to guide the motion patterns toward the specific targets (symmetry and smiling motions). The efficiency of training reinforcement learning algorithms is demonstrated by the reward values predicted using the learned model. The "proper" reward function must be defined for successful training reinforcement learning. The current work used two simple reward functions to train the finite element model of the face for symmetry and smile motion. For more realistic outcomes, a bioinspired reward function built from the bio-mechanical knowledge should be developed for reshaping the mechanism of the desired facial motion. Moreover, two the state-of-the-art RL methods (DDPG method and the successor TD3), which are off-policy algorithms and applicable for complex environments with continuous action spaces, were used to drive the face

toward the targeted motions from the activation of the facial muscles. Note that the use of these methods leads to the win of the Learn to Move competition [35]. The reward values during training model using DDPG algorithm seem noisier compared to that of training model using TD3 algorithm. This is due to the nature of DDPG algorithm when it updating the policy more often during training. In terms of reward predicted from the trained model, TD3 seems to have slightly better performance compared to DDPG.

One of the most important limitations of the present work deals with the sensitive nature of the hyperparameters of the physics-based face model. Further investigations should be done to take the uncertainties of these parameters into account to provide more reliable prediction outcomes. In fact, each parameter should be represented in a more generic format like interval or probability-based structures (e.g. probability density function (PDF); cumulative distribution function (CDF)) and then associated outcomes (i.e. muscle activation) should be estimated within a plausible range of values. However, taking the parameter uncertainty into account increases drastically the computational cost during the reinforcement learning process. Thus, more efficient uncertainty propagation algorithms should be investigated to scope with this constraint. Moreover, the present face model includes only 10 muscles. In particular, all parameters were set up for a generic model. Thus, a more detailed face model and patient-specific properties of the face tissues and structures should be taken into consideration from medical imaging toward a patient specific rehabilitation application. In particular, the increase of the number of muscles of interest will allow the modeling system to explore full muscle action patterns of the face. Thus, the present system could benefit from the FACS pattern for a given expression to converge quickly to the optimal solution and then other applications like speech synthesis or language learning could be investigated. Regarding the limitation of the used RL

approach, the use of only a deep neural network seems to be underestimated for the complex face motion coordination. As perspective, a multi-network approach should be investigated for a better coordination of the facial muscle activations and contractions. Finally, the coupling between RL and FE modeling frameworks requires the development of a specific communication protocol. In a further work, the developed information exchange protocol will be improved to provide a generic communication channel between the RL framework and any other powerful and dedicated FE modeling frameworks like Abaqus or Ansys to overcome the limitation of the current physics-based face model.

5. Conclusions

The present study explored the muscle excitation patterns by coupling reinforcement learning with a finite element model of the face. We developed, for the first time, a novel coupling scheme to integrate the finite element simulation into the reinforcement learning for facial motion learning. In particular, two state-of-the-art reinforcement learning algorithms (deep deterministic policy gradient (DDPG) and Twin-delayed DDPG (TD3)) were successfully applied and implemented to drive the simulations of symmetry-oriented and smile movements. Obtained results were in very good agreement with experimental observation. In fact, a better understanding of the facial muscle activation and coordination mechanism is of great clinical interest to guide the optimal rehabilitation strategy. The present work opens new avenues to achieve this challenging objective. As perspectives, this present workflow will be applied for facial palsy and facial transplantation patients to guide and optimize the functional rehabilitation program.

Acknowledgement

This work was financially supported by Sorbonne Center for Artificial Intelligence (SCAI).

495 **Compliance with ethical standards**

496 The authors declare that there are no ethical issues for the present work.

497 **References**

- 498 [1] Bogart, Kathleen R., Linda Tickle-Degnen, and Nalini Ambady. "Communicating
499 without the face: holistic perception of emotions of people with facial paralysis." *Basic and*
500 *applied social psychology* 36.4 (2014): 309-320.
- 501 [2] Magagna, Jeanne. "Communicating without words." *The Silent Child*. Routledge, 2018.
502 29-46.
- 503 [3] Fuller, Geraint, and Cathy Morgan. "Bell's palsy syndrome: mimics and
504 chameleons." *Practical Neurology* 16.6 (2016): 439-444.
- 505 [4] Grewal, D. S. "Atlas of Surgery of the Facial Nerve: An Otolaryngologist's
506 Perspective". *JAYPEE BROTHERS PUBLISHERS*, 2014.
- 507 [5] Haase, Daniel, et al. "Automated and objective action coding of facial expressions in
508 patients with acute facial palsy." *European Archives of Oto-Rhino-Laryngology* 272.5
509 (2015): 1259-1267.
- 510 [6] He, Shu, et al. "Quantitative analysis of facial paralysis using local binary patterns in
511 biomedical videos." *IEEE Transactions on Biomedical Engineering* 56.7 (2009): 1864-
512 1870.
- 513 [7] Robinson, Mara Wernick, et al. "Facial rehabilitation." *Operative Techniques in*
514 *Otolaryngology-Head and Neck Surgery* 23.4 (2012): 288-296.
- 515 [8] Jayatilake, Dushyantha, et al. "Robot assisted physiotherapy to support rehabilitation of
516 facial paralysis." *IEEE Transactions on Neural Systems and Rehabilitation*
517 *Engineering* 22.3 (2013): 644-653.

- 518 [9] Pileicikienė, Gaivile, et al. "A three-dimensional model of the human masticatory
519 system, including the mandible, the dentition and the temporomandibular
520 joints." *Stomatologija* 9.1 (2007): 27-32.s
- 521 [10] Erdemir, Ahmet, et al. "Model-based estimation of muscle forces exerted during
522 movements." *Clinical biomechanics* 22.2 (2007): 131-154.
- 523 [11] Zhang, Yu, Edmond C. Prakash, and Eric Sung. "Face alive." *Journal of Visual*
524 *Languages & Computing* 15.2 (2004): 125-160.
- 525 [12] Claes, Peter, et al. "Computerized craniofacial reconstruction: conceptual framework
526 and review." *Forensic science international* 201.1-3 (2010): 138-145.
- 527 [13] Mollemans, Wouter, et al. "Predicting soft tissue deformations for a maxillofacial
528 surgery planning system: from computational strategies to a complete clinical
529 validation." *Medical image analysis* 11.3 (2007): 282-301.
- 530 [14] Kim, Hyungmin, et al. "A new soft-tissue simulation strategy for cranio-maxillofacial
531 surgery using facial muscle template model." *Progress in biophysics and molecular*
532 *biology* 103.2-3 (2010): 284-291.
- 533 [15] Hannam, A. G. "Current computational modelling trends in craniomandibular
534 biomechanics and their clinical implications." *Journal of oral rehabilitation* 38.3 (2011):
535 217-234.
- 536 [16] Flynn, C., Stavness, I., Lloyd, J., & Fels, S. (2015). A finite element model of the face
537 including an orthotropic skin model under in vivo tension. *Computer methods in*
538 *biomechanics and biomedical engineering*, 18(6), 571-582.

- 539 [17] Yu, Chao, Jiming Liu, and Shamim Nemati. "Reinforcement learning in healthcare: A
540 survey." *arXiv preprint arXiv:1908.08796* (2019).
- 541 [18] Kormushev, Petar, Sylvain Calinon, and Darwin G. Caldwell. "Reinforcement
542 learning in robotics: Applications and real-world challenges." *Robotics* 2.3 (2013): 122-
543 148.
- 544 [19] Szita, István. "Reinforcement learning in games." *Reinforcement learning*. Springer,
545 Berlin, Heidelberg, 2012. 539-577.
- 546 [20] Sallab, Ahmad EL, et al. "Deep reinforcement learning framework for autonomous
547 driving." *Electronic Imaging* 2017.19 (2017): 70-76.
- 548 [21] Bueno, M. B., Nieto, X. G. I., Marqués, F., & Torres, J. (2017). Hierarchical object
549 detection with deep reinforcement learning. *Deep Learning for Image Processing*
550 *Applications*, 31(164), 3.
- 551 [22] Jonsson, A. (2019). Deep reinforcement learning in medicine. *Kidney Diseases*, 5(1),
552 18-22.
- 553 [23] Gottesman, Omer, et al. "Guidelines for reinforcement learning in healthcare." *Nature*
554 *medicine* 25.1 (2019): 16-18.
- 555 [24] Maia, Tiago V., and Michael J. Frank. "From reinforcement learning models to
556 psychiatric and neurological disorders." *Nature neuroscience* 14.2 (2011): 154-162.
- 557 [25] Nazari, Mohammad Ali, et al. "Simulation of dynamic orofacial movements using a
558 constitutive law varying with muscle activation." *Computer methods in biomechanics and*
559 *biomedical engineering* 13.4 (2010): 469-482.

- 560 [26] Bucki, Marek, Mohammad Ali Nazari, and Yohan Payan. "Finite element speaker-
561 specific face model generation for the study of speech production." *Computer methods in*
562 *biomechanics and biomedical engineering* 13.4 (2010): 459-467.
- 563 [27] John E. Lloyd, Ian Stavness, and Sidney Fels, "ArtiSynth: A fast interactive
564 biomechanical modeling toolkit combining multibody and finite element simulation", *Soft*
565 *Tissue Biomechanical Modeling for Computer Assisted Surgery*, pp. 355-394, Springer,
566 2012.
- 567 [28] Stavness, Ian, et al. "Coupled biomechanical modeling of the face, jaw, skull, tongue,
568 and hyoid bone." *3D multiscale physiological human*. Springer, London, 2014. 253-274.
- 569 [29] Jiang, Zeqing, et al. "A Cloud-Based Training and Evaluation System for Facial
570 Paralysis Rehabilitation." *2018 IEEE 16th International Conference on Industrial*
571 *Informatics (INDIN)*. IEEE, 2018.
- 572 [30] Abdi, Amir H., et al. "Reinforcement learning for high-dimensional continuous
573 control in biomechanics: an intro to artisynth-rl." *arXiv preprint arXiv:1910.13859* (2019).
- 574 [31] Fan, A. X., Dakpé, S., Dao, T. T., Pouletaut, P., Rachik, M., & Ho Ba Tho, M. C.
575 (2017). "MRI-based finite element modeling of facial mimics: a case study on the paired
576 zygomaticus major muscles." *Computer methods in biomechanics and biomedical*
577 *engineering*, 20(9), 919-928.
- 578 [32] Dao, T. T., Fan, A. X., Dakpe, S., Pouletaut, P., Rachik, M., & HO BA THO, M. C.
579 (2018). "Image-based skeletal muscle coordination: case study on a subject specific facial
580 mimic simulation." *Journal of Mechanics in Medicine and Biology*, 18(02), 1850020.

581 [33] K Nowakowski, P Carvalho, J B Six, Y Maillet, A T Nguyen, I Seghiri, L M'Pemba,
582 T Marcille, S T Ngo, T T Dao (2021). "Human locomotion with reinforcement learning
583 using bioinspired reward reshaping strategies." *Medical & Biological Engineering &*
584 *Computing*, 59(1), 243-256.

585 [34] Asri, Hiba, et al. "Big data in healthcare: Challenges and opportunities." *2015*
586 *International Conference on Cloud Technologies and Applications (CloudTech)*. IEEE,
587 2015.

588 [35] Song, Seungmoon, et al. "Deep reinforcement learning for modeling human
589 locomotion control in neuromechanical simulation." *Journal of NeuroEngineering and*
590 *Rehabilitation* 18.1 (2021): 1-17. <https://doi.org/10.1186/s12984-021-00919-y>

591 [36] Hamm, Jihun, et al. "Automated facial action coding system for dynamic analysis of
592 facial expressions in neuropsychiatric disorders." *Journal of neuroscience methods* 200.2
593 (2011): 237-256.

594 [37] Tian, Y-I., Takeo Kanade, and Jeffrey F. Cohn. "Recognizing action units for facial
595 expression analysis." *IEEE Transactions on pattern analysis and machine intelligence* 23.2
596 (2001): 97-115.

597 [38] Choi, Kang Young. "Analysis of facial asymmetry." *Archives of craniofacial*
598 *surgery* 16.1 (2015): 1

599 [39] Eskes, Merijn, et al. "Simulation of facial expressions using person-specific sEMG
600 signals controlling a biomechanical face model." *International journal of computer*
601 *assisted radiology and surgery* 13.1 (2018): 47-59.

- [40] Nguyen, Tan-Nhu, et al. "Kinect-driven patient-specific head, skull, and muscle network modelling for facial palsy patients." *Computer Methods and Programs in Biomedicine* 200 (2021): 105846.
- [41] Fujimoto, Scott, Herke Hoof, and David Meger. "Addressing function approximation error in actor-critic methods." *International conference on machine learning*. PMLR, 2018.

AUTHOR BIOGRAPHIES



Duc-Phong NGUYEN is currently a Ph.D student in Biomechanic Engineering at the Uninversity of Technology of Compiègne (France). His current research interest is facial recognition and rehabilitation for medical computer aided system diagnosis.



Marie-Christine HO BA THO is Full Professor in Mechanics since 1998 at the Uninversity of Technology of Compiègne (France). She is currently Head of Research at UTC. Her research work concerns Biomechanics of the musculoskeletal system and the modelling of uncertainties of biomechanics data.



Tien Tuan Dao is Full Professor of Biomedical Engineering and Biomechanics at Centrale Lille Institut, France. His research interests concern computational biomechanics, knowledge and system engineering, and in silico medicine.

